

2



AD-A249 068



FATIGUE CRACK GROWTH IN AerMet 100 STEEL

Eun U. Lee
Air Vehicle and Crew Systems Technology Department (Code 6063)
NAVAL AIR DEVELOPMENT CENTER
Warminster, PA 18974-5000

18 OCTOBER 1991

PHASE REPORT

Approved for Public Release; Distribution Is Unlimited

DTIC
ELECTE
APR 13 1992
S B D

Prepared for
Air Vehicle and Crew Systems Technology Department (Code 606)
NAVAL AIR DEVELOPMENT CENTER
Warminster, PA 18974-5000

92-09193



92-09193

NOTICES

REPORT NUMBERING SYSTEM — The numbering of technical project reports issued by the Naval Air Development Center is arranged for specific identification purposes. Each number consists of the Center acronym, the calendar year in which the number was assigned, the sequence number of the report within the specific calendar year, and the official 2-digit correspondence code of the Command Officer or the Functional Department responsible for the report. For example: Report No. NADC-88020-60 indicates the twentieth Center report for the year 1988 and prepared by the Air Vehicle and Crew Systems Technology Department. The numerical codes are as follows:

CODE	OFFICE OR DEPARTMENT
00	Commander, Naval Air Development Center
01	Technical Director, Naval Air Development Center
05	Computer Department
10	AntiSubmarine Warfare Systems Department
20	Tactical Air Systems Department
30	Warfare Systems Analysis Department
40	Communication Navigation Technology Department
50	Mission Avionics Technology Department
60	Air Vehicle & Crew Systems Technology Department
70	Systems & Software Technology Department
80	Engineering Support Group
90	Test & Evaluation Group

PRODUCT ENDORSEMENT — The discussion or instructions concerning commercial products herein do not constitute an endorsement by the Government nor do they convey or imply the license or right to use such products.

Reviewed By: J. Waldman Date: 31 Jan 92
Branch Head

Reviewed By: [Signature] Date: 5 Feb 92
Division Head

Reviewed By: J. H. [Signature] Date: 2 Feb 92
Director/Deputy Director

REPORT DOCUMENTATION PAGE

Form Approved
OMB No 0704-0188

Public reporting burden for this collection of information is estimated to average 1 hour per response, including the time for reviewing instructions, searching existing data sources, gathering and maintaining the data needed, and completing and reviewing the collection of information. Send comments regarding this burden estimate or any other aspect of this collection of information, including suggestions for reducing this burden, to Washington Headquarters Services, Directorate for Information Operations and Reports, 1215 Jefferson Davis Highway, Suite 1204, Arlington, VA 22202-4302 and to the Office of Management and Budget, Paperwork Reduction Project (0704-0188), Washington, DC 20503

1. AGENCY USE ONLY (Leave blank)	2. REPORT DATE 18 October 1991	3. REPORT TYPE AND DATES COVERED Phase	
4. TITLE AND SUBTITLE Fatigue Crack Growth in AerMet 100 Steel		5. FUNDING NUMBERS	
6. AUTHOR(S) Eun U. Lee		7. PERFORMING ORGANIZATION NAME(S) AND ADDRESS(ES) Air Vehicle and Crew Systems Technology Department (Code 6063) NAVAL AIR DEVELOPMENT CENTER Warminster, PA 18974-5000	
8. PERFORMING ORGANIZATION REPORT NUMBER NADC-91111-60		9. SPONSORING / MONITORING AGENCY NAME(S) AND ADDRESS(ES) Air Vehicle and Crew Systems Technology Department (Code 6063) NAVAL AIR DEVELOPMENT CENTER Warminster, PA 18974-5000	
10. SPONSORING / MONITORING AGENCY REPORT NUMBER		11. SUPPLEMENTARY NOTES	
12a. DISTRIBUTION / AVAILABILITY STATEMENT Approved for Public Release; Distribution is Unlimited.		12b. DISTRIBUTION CODE	
13. ABSTRACT (Maximum 200 words) The fatigue behavior of a newly developed landing gear steel, AerMet 100, was studied. In this study, the fatigue tests were performed under constant amplitude loading for stress ratios $R = 0.1, 0.5,$ and 0.8 in dry nitrogen gas and a 3.5% NaCl solution at room temperature. The fatigue crack growth resistance of the AerMet 100 Steel is superior to that of the 300M steel, which has been widely used for aircraft landing gears. Within the employed range of stress ratios, the greater the stress ratio, the smaller is the threshold stress intensity range for fatigue crack growth ΔK_{th} and the greater is the fatigue crack growth rate da/dN for lower ΔK . For higher ΔK , however, the da/dN values of different stress ratios are similar in both environments. The ΔK_{th} is greater and da/dN is smaller for lower ΔK in a 3.5% NaCl solution than in dry nitrogen gas, whereas the da/dN values are quite close for higher ΔK in both			
14. SUBJECT TERMS fatigue behavior, landing gear steel, AerMet 100, constant amplitude loading, stress ratio, crack growth		15. NUMBER OF PAGES	
17. SECURITY CLASSIFICATION OF REPORT Unclassified		16. PRICE CODE	
18. SECURITY CLASSIFICATION OF THIS PAGE Unclassified	19. SECURITY CLASSIFICATION OF ABSTRACT Unclassified	20. LIMITATION OF ABSTRACT UL	

Unclassified

SECURITY CLASSIFICATION OF THIS PAGE

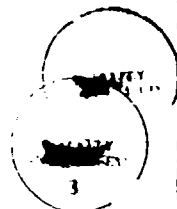
13. ABSTRACT (Cont'd)

environments. This feature is attributable to corrosion-product-induced crack closure.

CONTENTS

	Page
FIGURES	iv
ABSTRACT	v
ACKNOWLEDGEMENTS	vi
INTRODUCTION	1
EXPERIMENTAL PROCEDURE	1
MATERIAL AND SPECIMEN PREPARATION	1
FATIGUE TEST	2
MICROSTRUCTURAL AND FRACTOGRAPHIC EXAMINATION	2
RESULTS	2
FATIGUE CRACK GROWTH	2
MICROSTRUCTURE	2
FRACTOGRAPHY	3
DISCUSSION	3
CONCLUSION	4
REFERENCES	5

Accession For	
NTIS GRA&I	<input checked="" type="checkbox"/>
DTIC TAB	<input type="checkbox"/>
Unannounced	<input type="checkbox"/>
Justification	
By _____	
Distribution/	
Availability Codes	
Dist	Avail and/or Special
A-1	
	1



NADC-91111-60

FIGURES

Figure		Page
1	Variation of Fatigue Crack Growth Rate, da/dN , with Stress Intensity Range, ΔK , for Stress Ratio $R = 0.1, 0.5,$ and 0.8 in Dry Nitrogen Gas	6
2	Variation of Fatigue Crack Growth Rate, da/dN , with Stress Intensity Range, ΔK , for Stress Ratio $R = 0.1, 0.5,$ and 0.8 in a 3.5% NaCl Solution	7
3	Variation of Threshold Stress Intensity Range for Fatigue Crack Growth, ΔK_{th} , with Stress Ratio, R , in Dry Nitrogen Gas and a 3.5% NaCl Solution	8
4	Variation of Fatigue Crack Growth Rate, da/dN , with Stress Intensity Range, ΔK , for Stress Ratio $R = 0.1$ in Dry Nitrogen Gas and a 3.5% NaCl Solution	9
5	Variation of Fatigue Crack Growth Rate, da/dN , with Stress Intensity Range, ΔK , for Stress Ratio $R = 0.5$ in Dry Nitrogen Gas and a 3.5% NaCl Solution	10
6	Variation of Fatigue Crack Growth Rate, da/dN , with Stress Intensity Range, ΔK , for Stress Ratio $R = 0.8$ in Dry Nitrogen Gas and a 3.5% NaCl Solution	11
7	Micrograph of Specimen Material, AerMet 100 Steel	12
8	Fractographs of Specimen Fatigue-Tested in Dry Nitrogen Gas	13
9	Fractographs of Specimen Fatigue-Tested in a 3.5% NaCl Solution	14
10	Variation of Fatigue Crack Growth Rate, da/dN , with Stress Intensity Range, ΔK , for AerMet 100 and 300M Steels in Inert Environments	15
11	Variation of Fatigue Crack Growth Rate, da/dN , with Stress Intensity Range, ΔK , for AerMet 100 and 300M Steels in Corrosive Environments	16

ABSTRACT

The fatigue behavior of a newly developed landing gear steel, AerMet 100, was studied. In this study, the fatigue tests were performed under constant amplitude loading for stress ratios $R = 0.1, 0.5,$ and 0.8 in dry nitrogen gas and a 3.5% NaCl solution at room temperature.

The fatigue crack growth resistance of the AerMet 100 steel is superior to that of the 300M steel, which has been widely used for aircraft landing gears.

Within the employed range of stress ratios, the greater the stress ratio, the smaller is the threshold stress intensity range for fatigue crack growth ΔK_{th} and the greater is the fatigue crack growth rate da/dN for lower ΔK . For higher ΔK , however, the da/dN values of different stress ratios are similar in both environments.

The ΔK_{th} is greater and da/dN is smaller for lower ΔK in a 3.5% NaCl solution than in dry nitrogen gas, whereas the da/dN values are quite close for higher ΔK in both environments. This feature is attributable to corrosion-product-induced crack closure.

NADC-91111-60

ACKNOWLEDGEMENTS

This study was supported by the ONT 6.2 Airborne Materials Block, P.E. 62234N.

The author is grateful to Carpenter Technology Corp. for providing and heat-treating the specimen material, AerMet 100 steel, Mr. W. F. Warden for the fatigue testing, Mr. W. Weist for the SEM work, and Mr. E. Deesing for the microstructural examination.

INTRODUCTION

Carrier-based aircraft landing gears demand tough, corrosion resistant materials in order to achieve higher performance and greater reliability at minimum life-cycle cost. The performance and reliability can be determined from the fatigue behavior under testing conditions that simulate those encountered in actual service. Therefore, the fatigue behavior of potential materials for landing gears should be thoroughly investigated prior to their actual use.

For the past 20 years, 300M steel was accepted as the standard material for landing gears because of its high ultimate tensile strength. Recently, a newly developed landing gear steel, AerMet 100, has been found to be potentially better than 300M steel due to its greater fracture toughness and better resistance to stress corrosion cracking and hydrogen embrittlement. However, its fatigue behavior has not yet been fully characterized.

In this study, the fatigue behavior of AerMet 100 steel is investigated under constant amplitude loading in inert and corrosive environments. The fatigue behavior under spectrum loading will be studied in the near future.

EXPERIMENTAL PROCEDURE

MATERIAL AND SPECIMEN PREPARATION

The AerMet 100 steel used in this study was received from Carpenter Technology Corp. in the form of a 1 1/4 x 3 3/8 x 12 in. slab, which was initially forged at 1850°F and annealed at 1250°F for 16 hours. Its nominal chemical composition in weight percent is shown below.

C - - - 0.23	Ni - - - 11.1	Cr - - - 3.1
Co - - - 13.4	Mo - - - 1.2	Fe - - - Balance

The specimen material was subjected to the following heat-treatment.

1. solution treatment at 1625°F for 1 hour and air cooling
2. deep freezing at -100°F for 1 hour and air warming
3. aging at 900°F for 5 hours and air cooling

Its mechanical properties in the longitudinal orientation are:

Yield Strength (ksi)	250
Tensile Strength (ksi)	285
Elongation (%)	14
Reduction of Area (%)	65
K _{IC} (ksi √in)	115

After the heat-treatment, compact-type (CT) specimens of width W = 1.0 in., thickness B = 0.25 in., and notch-tip length a_n = 0.20 in. were prepared in the L-T orientation by the process of Electro Discharge Machining.

FATIGUE TEST

The fatigue tests were conducted using CT specimens on a 100,000 lb closed-loop servo-hydraulic Materials Testing System (MTS) machine, operating under constant amplitude loading at a cyclic frequency of 10 Hz (sine wave). Stress ratios ($R = \text{minimum stress}/\text{maximum stress}$) of 0.1, 0.5, and 0.8 were employed in controlled ambient temperature environments of dry nitrogen gas and a 3.5% NaCl solution in distilled water. Testing in dry nitrogen gas was carried out in a Plexiglas environmental chamber, which totally enclosed the specimen. Oil free nitrogen gas was dried to 5% relative humidity by passing through Drierite (CaSO_4) prior to entering the environmental chamber. A 3.5% NaCl solution environment was made by capillary-wetting of a wick. Its one end filled up the notch-tip of a CT specimen and the other end was in a bottle of a 3.5% NaCl solution in distilled water.

Crack length was continuously monitored employing the DC electrical potential drop method and it was also checked visually. Near-threshold crack growth rates were obtained under decreasing ΔK (load shedding) condition with K-gradient $C = 3.5 \text{ in}^{-1}$.

MICROSTRUCTURAL AND FRACTOGRAPHIC EXAMINATION

The microstructure of the specimen material was examined with an optical microscope after etching in a solution of 10 gm of sodium meta-bisulfite in 100 ml of distilled water.

The fracture surface morphologies of the specimen were examined with an AMR 100 scanning electron microscope operated at an accelerated voltage of 20 kV.

RESULTS

FATIGUE CRACK GROWTH

The results of this study indicate that the fatigue behavior of AerMet 100 steel is predominantly affected by stress ratio and environment.

1. Effect of Stress Ratio

The variation of fatigue crack growth rate da/dN with stress ratio R for dry nitrogen gas and a 3.5% NaCl solution environment is shown in Figs. 1 and 2. For the fatigue tests in both environments, the fatigue crack growth rates above 10^{-6} in/cycle are largely unaffected by stress ratio. On the other hand, at near-threshold levels, increasing stress ratio reduces the threshold stress intensity range for fatigue crack growth ΔK_{th} and increases the fatigue crack growth rate da/dN . The variation of ΔK_{th} with R is shown in Fig. 3.

2. Effect of Environment

The fatigue crack growth behavior in dry nitrogen gas and a 3.5% NaCl solution is compared for stress ratios $R = 0.1, 0.5, \text{ and } 0.8$ in Figs. 4 - 6, respectively. At low da/dN below 10^{-6} in/cycle or near-threshold levels, da/dN is greater and ΔK_{th} is smaller in dry nitrogen gas than in a 3.5% NaCl solution for all stress ratios employed. However, at high da/dN levels above 10^{-6} in/cycle, the da/dN values for a given ΔK are quite close in both of the environments, indicating little effect of environment on da/dN .

MICROSTRUCTURE

The microstructure consists mostly of fine tempered martensite plates, Fig. 7.

FRACTOGRAPHY

The fractographs of the specimen, fatigue-tested in dry nitrogen gas, show patches of striations with some secondary cracks in the fatigue crack growth zone and dimples in the overload fracture zone, Fig. 8. There is no detectable indication of corrosion deposit in any part of the fracture surface.

After fatigue-testing in a 3.5% NaCl solution, except for the final fatigue crack growth zone of high da/dN and the adjacent zone of overload fracture, the fracture surface is covered by corrosion products with mud-cracks, Fig. 9. Patches of striations with secondary cracks are observable in the final fatigue crack growth zone and dimples in the overload fracture zone.

DISCUSSION

It is interesting to compare the fatigue crack growth behavior of AerMet 100 and 300M steels, the latter of which has been widely used for aircraft landing gears. The respective plots of da/dN vs. ΔK for both steels in inert and corrosive environments are shown in Figs. 10 and 11. The testing conditions for the 300M steel (1) are not exactly identical to those in the current study on AerMet 100 steel. The inert environment is low-humidity-air for the 300M steel, and dry nitrogen gas for the AerMet 100 steel. The corrosive environment is simulated-sea-water for the 300M Steel, and a 3.5% NaCl solution for the AerMet 100 steel. The value of ΔK_{th} can not be found for the 300M steel from either of the figures. In the range of intermediate da/dN , there is little difference in fatigue crack growth rate for either environment. However, in the range of higher da/dN , the da/dN is drastically larger for the 300M steel than for the AerMet 100 steel, resulting in an earlier catastrophic fracture of the 300M steel under a given fatigue condition. This inferior fatigue crack growth resistance of the 300M steel is attributed to its inferior fracture toughness ($K_{IC} = 55 \text{ ksi}\sqrt{\text{in}}$) and its much smaller critical crack size, compared to those for the AerMet 100 steel ($K_{IC} = 115 \text{ ksi}\sqrt{\text{in}}$).

The present results show that environment and stress ratio can greatly influence the fatigue crack growth rates and ΔK_{th} at near-threshold stress intensities. The dry nitrogen gas environment accelerates near-threshold crack growth rates and reduces ΔK_{th} values relative to a 3.5% NaCl solution in distilled water. Furthermore, ΔK_{th} decreases more markedly with increasing stress ratio in a 3.5% NaCl solution than in dry nitrogen gas, as shown in Fig. 3. In each environment, there is an approximately linear relationship between the values of ΔK_{th} and R , in agreement with Stewart's observation (2). However, the effects are considerably reduced at higher stress intensities (ΔK greater than $10 \text{ ksi}\sqrt{\text{in}}$).

Similar features of environmental and stress ratio effects have also been reported by other workers, confirming the present results. Testing ASTM A533 B-1 steel, Paris et al (3) observed that the near-threshold fatigue crack growth rates and the ΔK_{th} values are greater and lower, respectively, in a distilled water environment than in air at room temperature. They also reported that for crack growth rates above $5 \times 10^{-6} \text{ in/cycle}$, the distilled water environment cracking rate begins to exceed that in the air for an equivalent ΔK . In the test of 3NiCrMoV steel, Stewart (2) demonstrated that in dry gaseous environments of hydrogen, air, and argon and at low stress ratio, ΔK_{th} values are much lower than in moist laboratory air. On the other hand, at high stress ratio ($R = 0.88 - 0.92$), ΔK_{th} values were found to be generally insensitive to environment. Ritchie et al (4) studied the near-threshold fatigue crack growth in a 2.25Cr - 1Mo pressure vessel steel in moist air, dry hydrogen gas, and dry argon gas, and reported the following. Near-threshold crack growth rates, in addition to showing a marked sensitivity to stress ratio, are significantly enhanced in the dry gaseous environments compared to moist air.

A rationale for the effect of environment and stress ratio on fatigue crack growth rate and ΔK_{th} value can be found in terms of a crack closure concept (5). Elber (5) originally suggested that crack closure may occur at positive loads in a tension-tension fatigue cycle as a result of plastic deformation produced

In the wake of a fatigue crack. This is known as plasticity-induced crack closure. This reduces the applied stress intensity range to a lower effective value, ΔK_{eff} , actually experienced at the crack tip. Crack closure has also been known to be induced by corrosion products formed within growing cracks. This is known as corrosion-product-induced or oxide-induced crack closure. A number of previous investigators, notably Paris et al (3), Tu and Seth (6), Skelton and Halgh (7), Stewart (2), and Suresh and Ritchie (4,8), have suggested the possibility of crack closure due to corrosion products influencing near-threshold crack growth rates and ΔK_{th} values. In a corrosive environment, corrosion products are formed within the fatigue crack, thickened at low stress ratios, and continuously broken and reformed behind the crack tip due to repeated contact between the crack surfaces. The presence of such corrosion products in the crack will increase the load in the fatigue cycle at which crack closure occurs. Therefore, the effective stress intensity range ΔK_{eff} will be lower than that applied, leading to lower crack growth rates and higher apparent ΔK_{th} values. However, as stress ratio is increased, less crack closure occurs thereby increasing crack growth rates and lowering ΔK_{th} values (9).

Considering the crack growth characteristics and formation of corrosion product on the crack surface during fatigue loading in a 3.5% NaCl solution, observed in this study, the near-threshold fatigue crack growth behavior in the corrosive environment is attributed to a mechanism involving corrosion-product-induced crack closure.

CONCLUSION

Based on a study of fatigue crack growth in AerMet 100 steel, tested in dry nitrogen gas and a 3.5% NaCl solution, the following conclusions can be drawn:

1. The fatigue crack growth resistance of the AerMet 100 steel is superior to that of the 300M steel in inert and corrosive environments.
2. The significant features of fatigue crack growth in the AerMet 100 steel are:
 - a. Near-threshold fatigue crack growth rates, below 10^{-6} in/cycle, are faster in dry nitrogen gas than in a 3.5% NaCl solution.
 - b. For each of the employed stress ratios, $R = 0.1, 0.5,$ and $0.8,$ the ΔK_{th} value is less in dry nitrogen gas than in a 3.5% NaCl solution.
 - c. The larger the stress ratio, the greater is the near-threshold fatigue crack growth rate and the smaller is the ΔK_{th} value in both environments.
 - d. At high fatigue crack growth rates, above 10^{-6} in/cycle, the effects of environment and stress ratio are substantially reduced.
 - e. The near-threshold fatigue crack growth behavior in a 3.5% NaCl solution is attributed to a mechanism involving corrosion-product-induced crack closure.

REFERENCES

1. Gallagher, J., "Damage Tolerant Design Handbook," Metals and Ceramics Information Center, Battelle Columbus Laboratories, Columbus, OH, v. 2, 1983, p. 6.23-15 and 6.23-21.
2. Stewart, A.T., "The Influence of Environment and Stress Ratio on Fatigue Crack Growth at Near Threshold Stress Intensities in Low-Alloy Steels," Engineering Fracture Mechanics, v. 13, 1980, pp. 463-478.
3. Paris, P.C., Bucci, R.J., Wessel, E.T., Clark, W.G., and Mager, T. R., "Extensive Study of Low Fatigue Crack Growth Rates in A533 and A508 Steels," Stress Analysis and Growth of Cracks, ASTM STP 513, American Society for Testing and Materials, 1972, pp. 141-176.
4. Ritchie, R.O., Suresh, S., and Moss, C.M., "Near-Threshold Fatigue Crack Growth in 2 1/4Cr - 1Mo Pressure Vessel Steel in Air and Hydrogen," Journal of Engineering Materials and Technology, Transactions of the ASME, v. 102, 1980, pp. 293-299.
5. Elber, W., "The Significance of Fatigue Crack Closure," Damage Tolerance in Aircraft Structures, ASTM STP 486, American Society for Testing and Materials, 1971, pp. 230-242.
5. Tu, L.K.L., and Seth, B.B. "Threshold Corrosion Fatigue Crack Growth in Steels," Journal of Testing and Evaluation, v. 6, 1978, pp. 66-74.
7. Skelton, R.P. and Haigh, J.R., "Fatigue Crack Growth Rates and Thresholds in Steels under Oxidizing Conditions," Materials Science and Engineering, v. 36, 1978, pp. 17-25.
8. Suresh, S., Zamiski, G.F., and Ritchie, R.O., "Oxide-Induced Crack Closure: An Explanation for Near-Threshold Corrosion Fatigue Crack Growth Behavior," Metallurgical Transactions, v. 12A, 1981, pp. 1435-1443.
9. Schmidt, R.A. and Paris, P.C., "Threshold for Fatigue Crack Propagation and the Effects of Load Ratio and Frequency," Progress in Flaw Growth and Fracture Toughness Testing, ASTM STP 536, American Society for Testing and Materials, 1973, pp. 79-94.

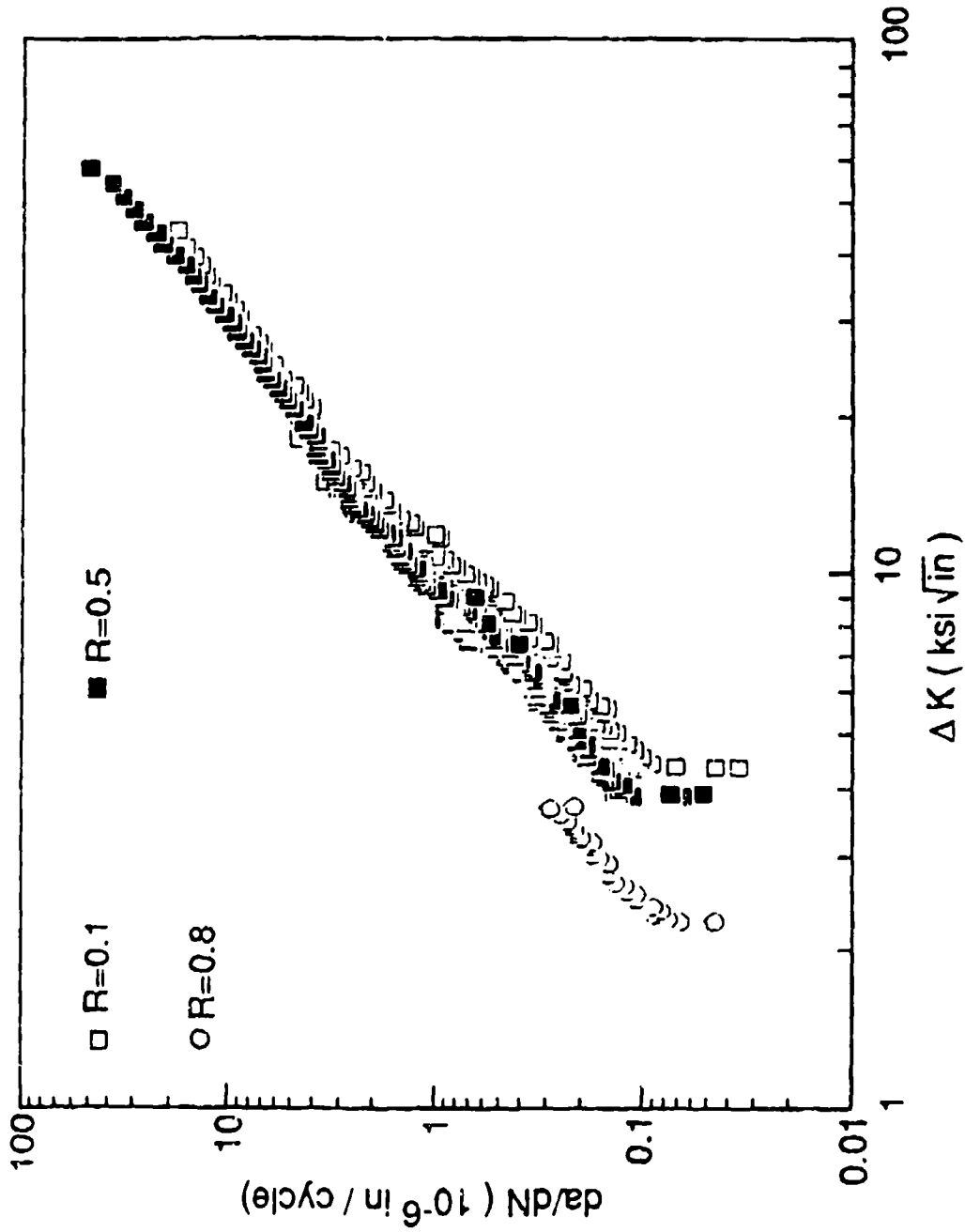


Figure 1. Variation of Fatigue Crack Growth Rate, da/dN , with Stress Intensity Range, ΔK , for Stress Ratio $R = 0.1, 0.5,$ and 0.8 in Dry Nitrogen Gas.

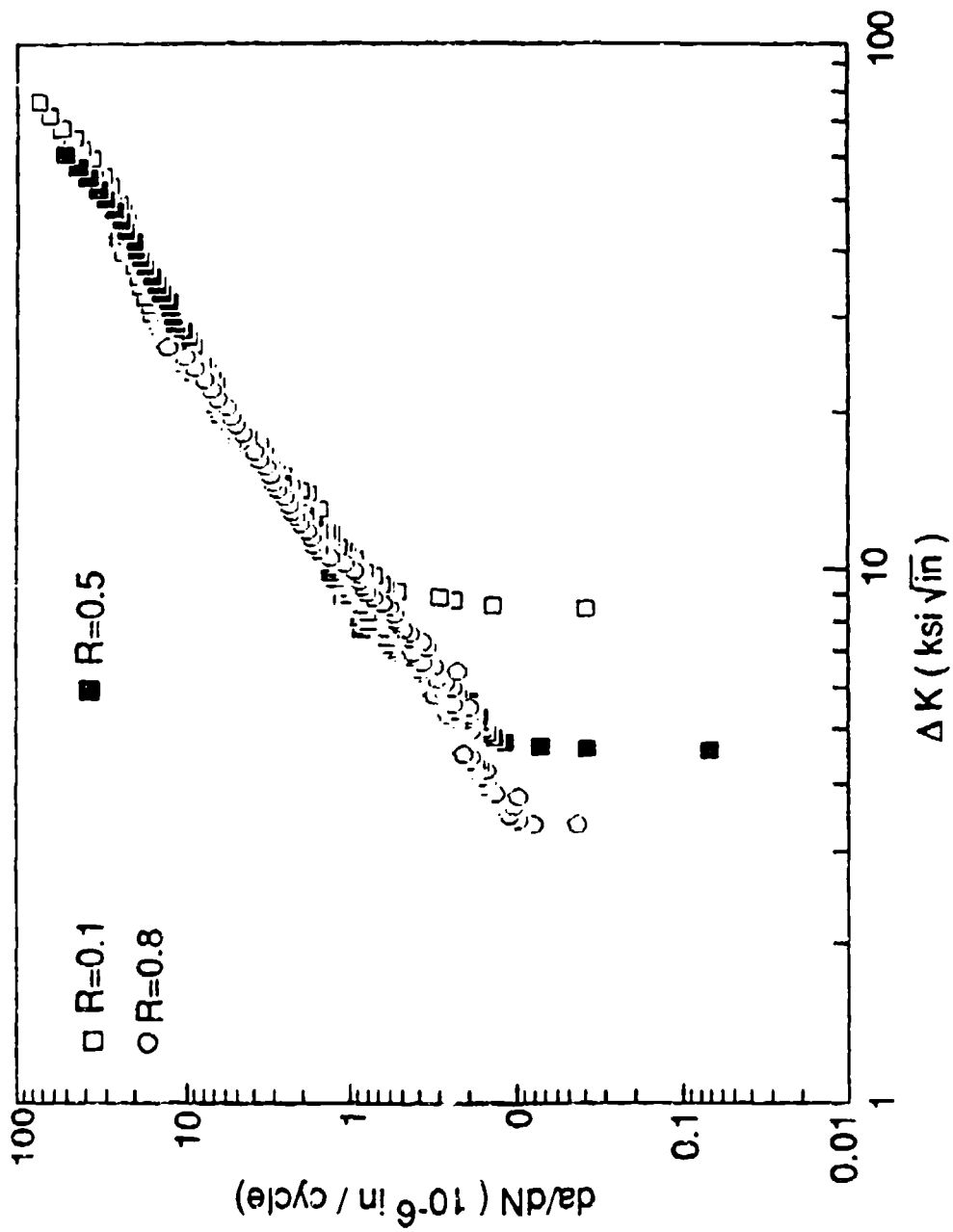


Figure 2. Variation of Fatigue Crack Growth Rate, da/dN , with Stress Intensity Range, ΔK , for Stress Ratio $R = 0.1, 0.5,$ and 0.8 in a 3.5% NaCl Solution.

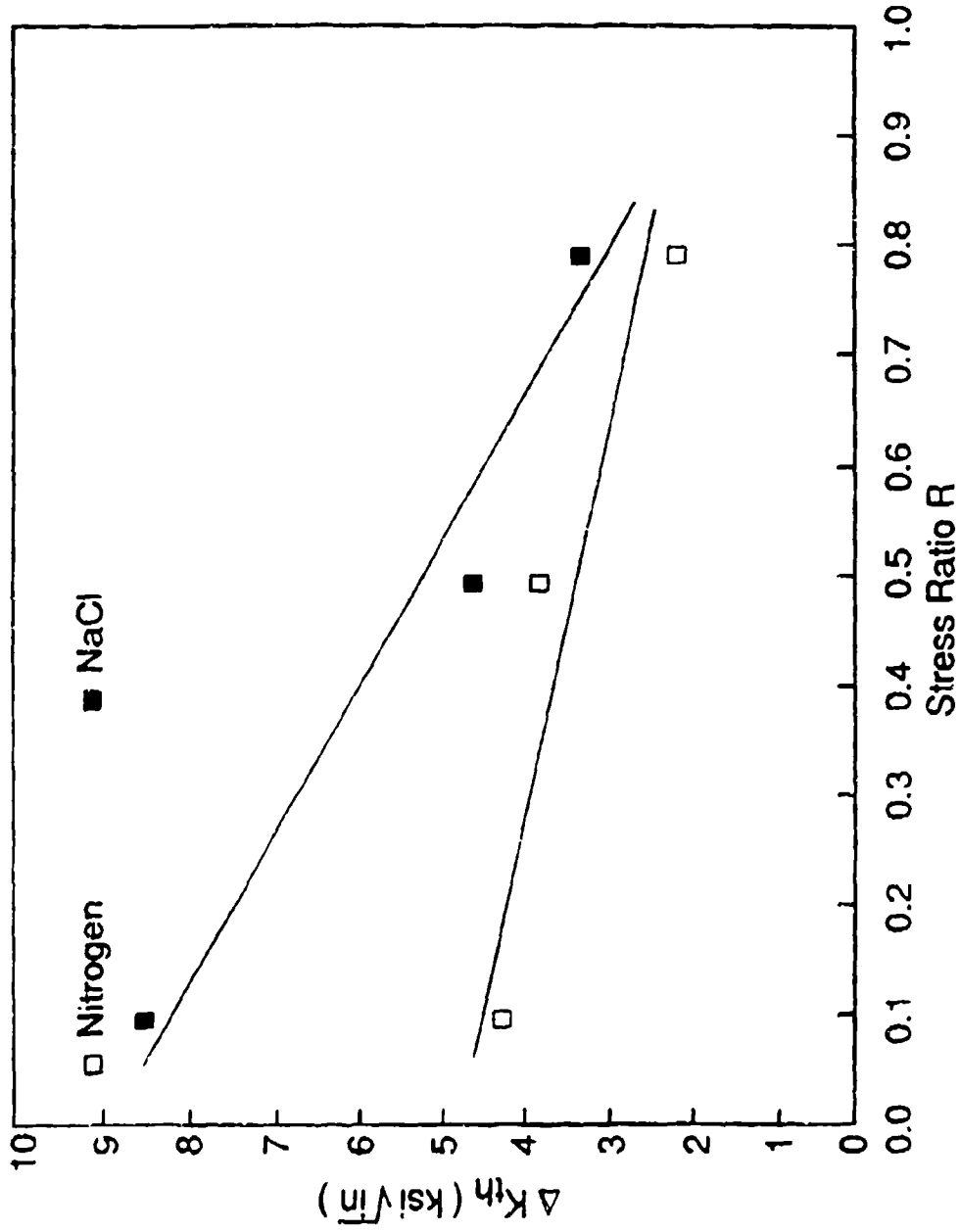


Figure 3. Variation of Threshold Stress Intensity Range for Fatigue Crack Growth, ΔK_{th} with Stress Ratio, R, in Dry Nitrogen Gas and a 3.5% NaCl Solution.

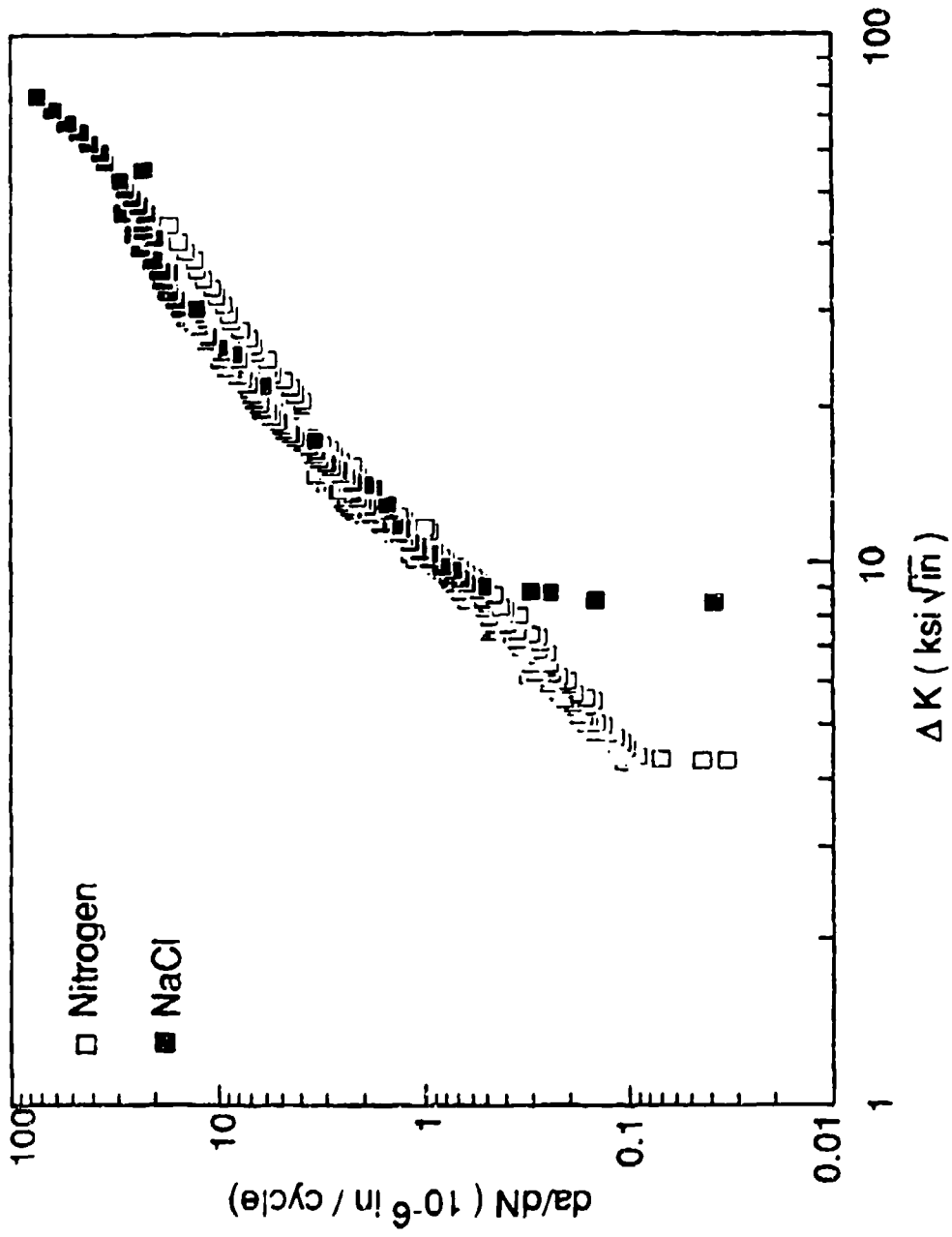


Figure 4. Variation of Fatigue Crack Growth Rate, da/dN , with Stress Intensity Range, ΔK , for Stress Ratio $R = 0.1$ in Dry Nitrogen Gas and a 3.5% NaCl Solution.

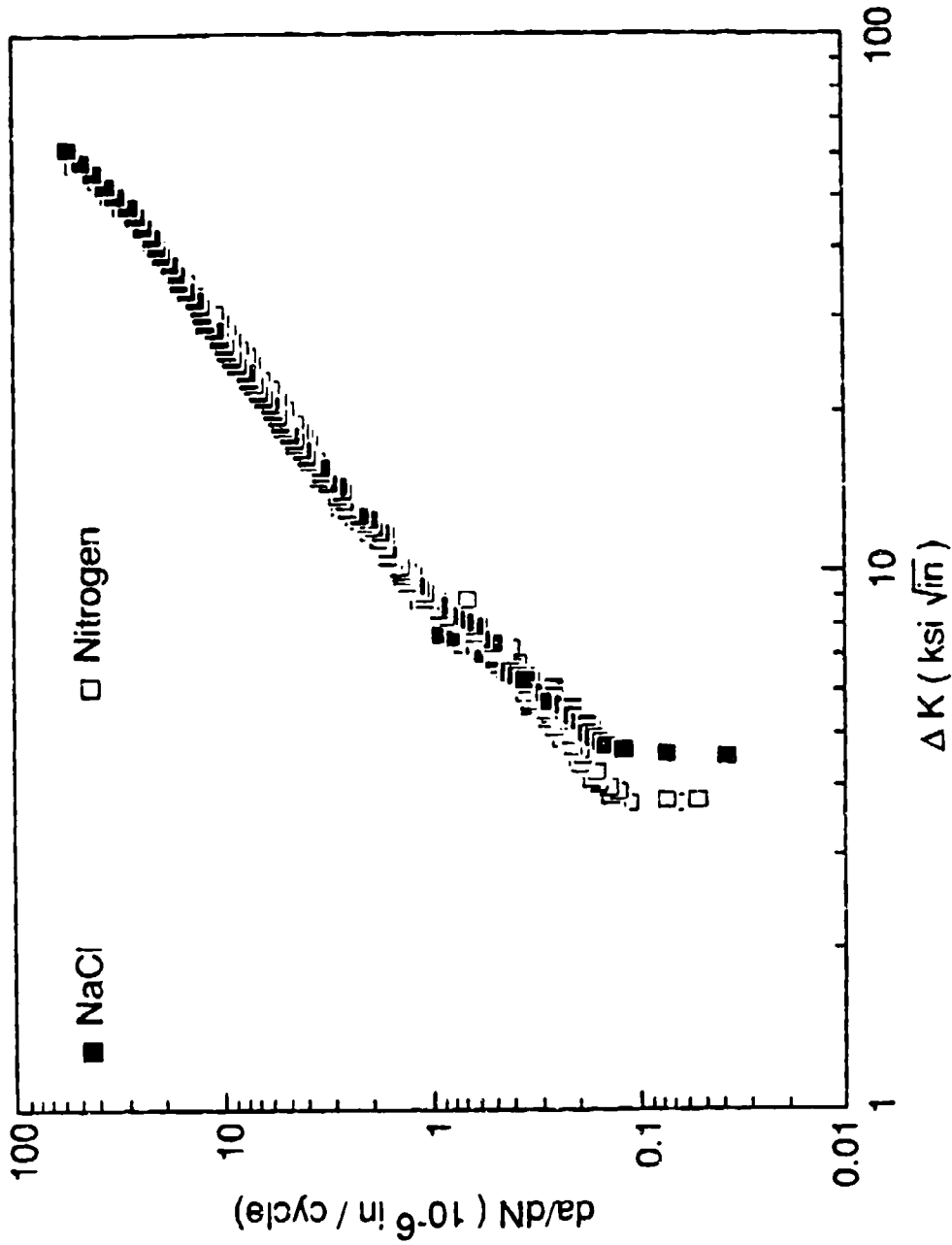


Figure 5. Variation of Fatigue Crack Growth Rate, da/dN , with Stress Intensity Range, ΔK , for Stress Ratio $R = 0.5$ in Dry Nitrogen Gas and a 3.5% NaCl Solution.

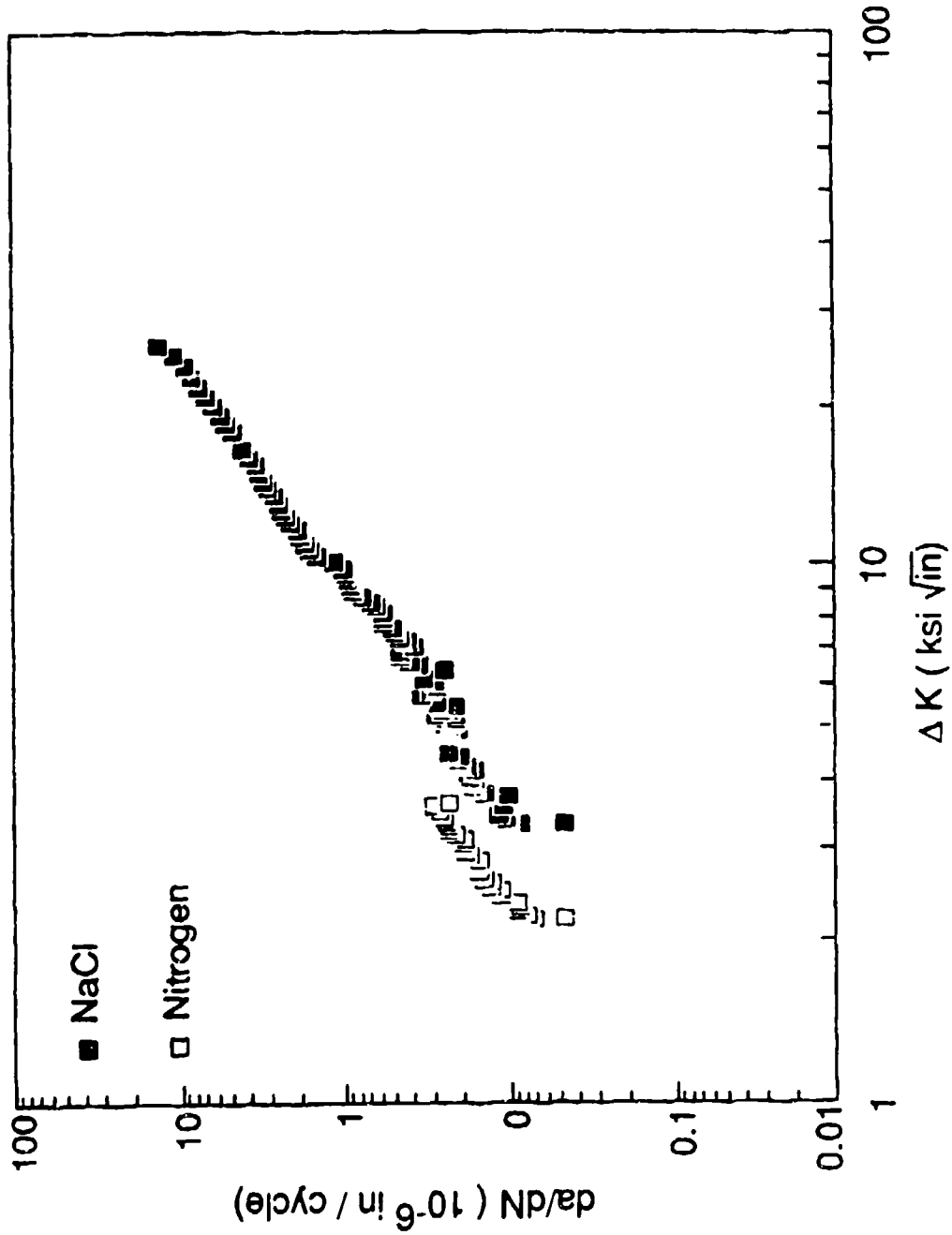


Figure 6. Variation of Fatigue Crack Growth Rate, da/dN , with Stress Intensity Range, ΔK , for Stress Ratio $R = 0.8$ in Dry Nitrogen Gas and a 3.5% NaCl Solution.

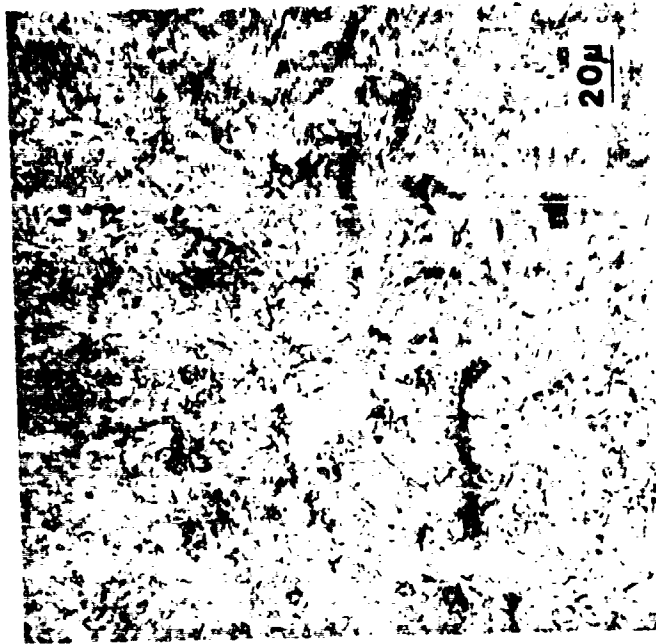
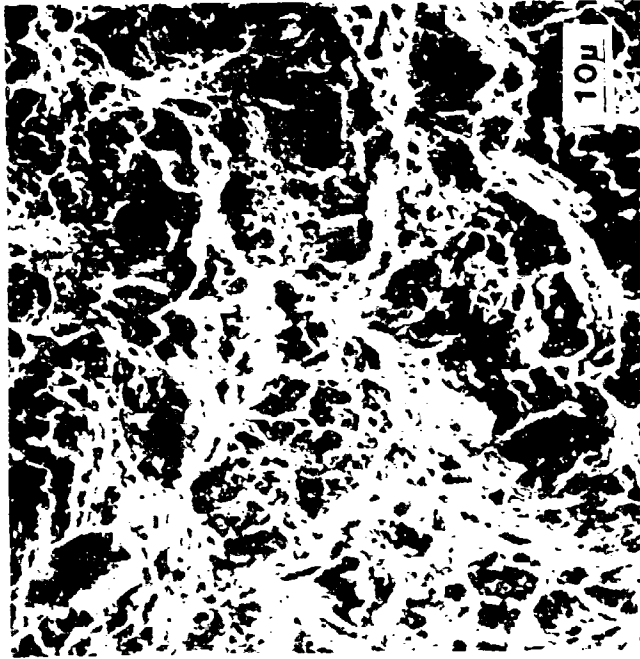


Figure 7. Micrograph of Specimen Material, AerMet 100 Steel.



(b) Overload Fracture Zone

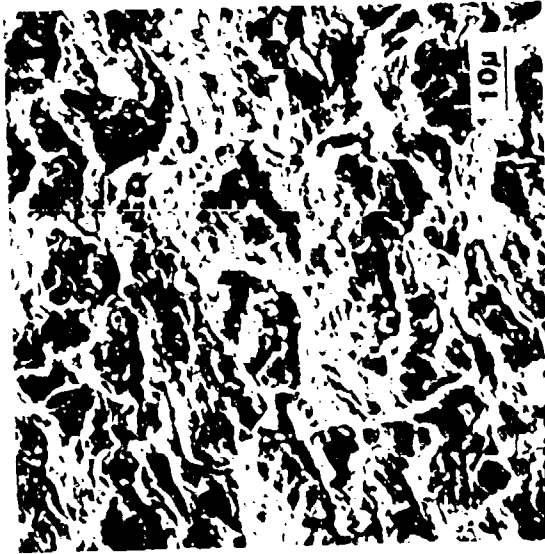


(a) Fatigue Crack Growth Zone

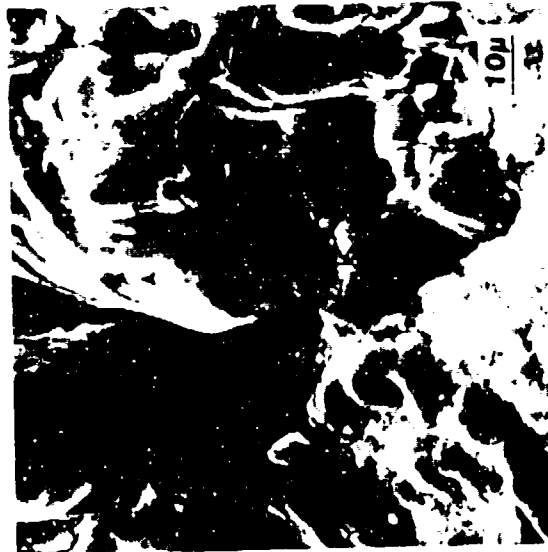
Figure 8. Fractographs of Specimen Fatigue-Tested in Dry Nitrogen Gas.



(c) Overload Fracture Zone



(b) Final Fatigue Crack Growth
Zone of High da/dN



(a) Fatigue Crack Growth Zone of
Low and Intermediate da/dN

Figure 9. Fractographs of Specimen Fatigue-Tested in a 3.5% NaCl Solution.

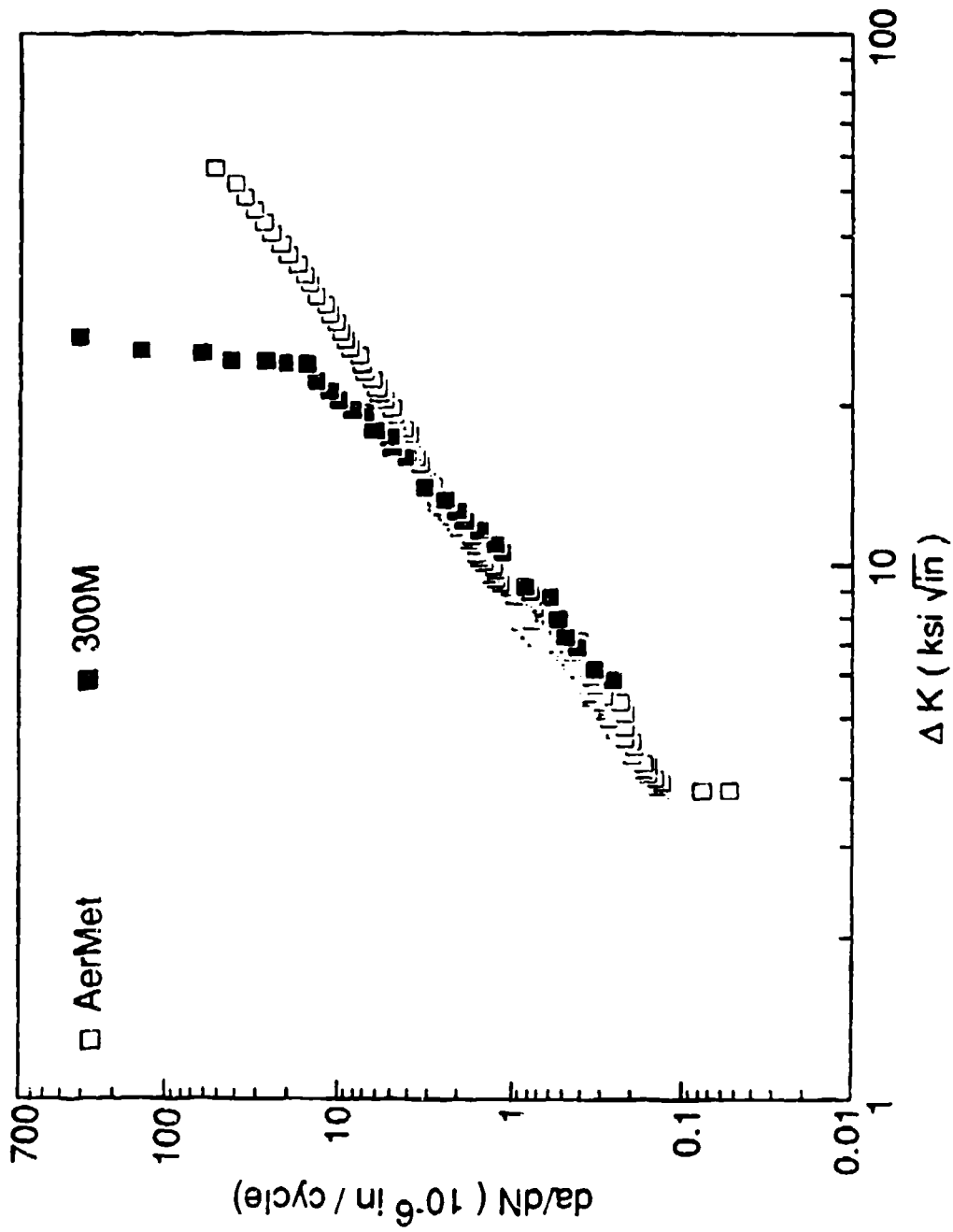


Figure 10. Variation of Fatigue Crack Growth Rate, da/dN , with Stress Intensity Range, ΔK , for AerMet 100 and 300M Steels in Inert Environments.

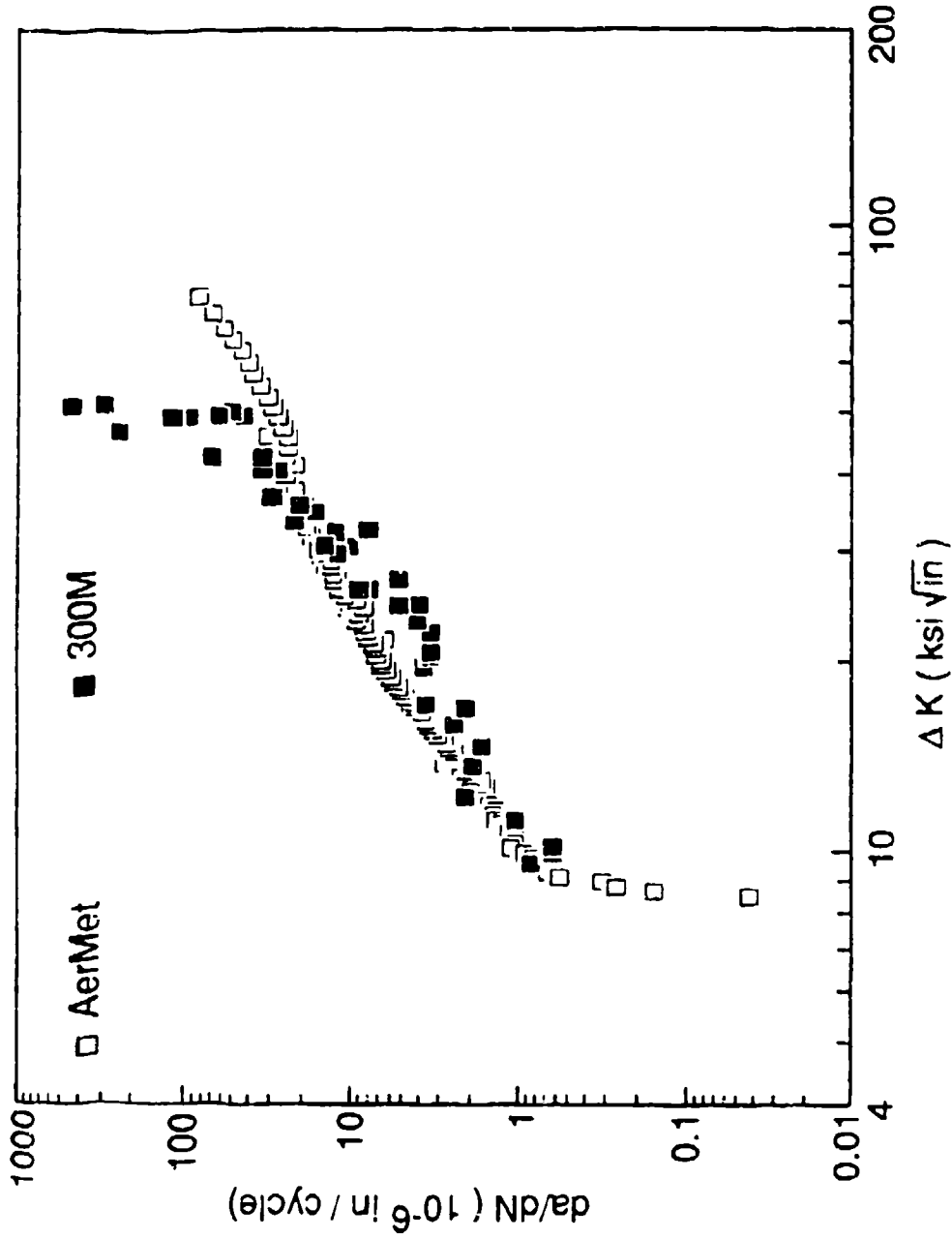


Figure 11. Variation of Fatigue Crack Growth Rate, da/dN , with Stress Intensity Range, ΔK , for AerMet 100 and 300M Steels in Corrosive Environments.

DISTRIBUTION LIST
Report No. NADC-91111-60

	No. of Copies
Naval Air Systems Command Washington, DC 20361-3030 (2 for AIR-530) (2 for AIR 931A) (1 for AIR-5302) (1 for AIR-5304)	6
Naval Sea Systems Command Washington, DC 20362	1
Naval Safety Center NAS, Norfolk, VA 23511	1
Naval Air Test Center Patuxent River, Md 20670-5304	1
Naval Research Laboratory 4555 Overlook Ave., SW Washington, DC 20375	1
David W. Taylor Naval Ship Research and Development Center Bethesda, MD 20084-5000	1
U.S. Air Force Systems Command Wright-Patterson AFB, OH 45433 (1 for FBR) (1 for FB) (1 for LLD) (1 for FYA) (1 for LAM) (1 for FBA) (1 for LPH)	7
Chief of Naval Research 800 N. Quincy St. Arlington, Va 22217-5000	1
Defense Technical Information Center ATTN: DTIC-FDAB Cameron Station BG5 Alexandria, VA 22304-6145	2
Center for Naval Analysis 4401 Fort Avenue P.O. Box 16268 Alexandria, VA 22302-0268	1

DISTRIBUTION LIST (Continued)
Report No. NADC-91111-60

	No. of Copies
Naval Air Development Center Warminster, PA 18974-5000 (20 for Code 6063) (2 for Code 8133)	22
Annapolis Laboratory David W. Taylor Naval Ship Research and Development Center Detachment Annapolis, MD 21402-1198	1
Naval Aviation Depot Naval Air Station Code 340 Alameda, CA 94501-5201	1
Naval Aviation Depot Marine Corps Air Station Code 340 Cherry Point, NC 28533-5030	1
Naval Aviation Depot Naval Air Station Code 340 Jacksonville, FL 32212	1
Naval Aviation Depot Naval Air Station Code 340 Norfolk, VA 23511-5899	1
Naval Aviation Depot North Island Code 340 Pensacola, FL 32508-5300	1
Naval Aviation Depot Naval Air Station Code 340 San Diego, CA 92135-5112	1
Naval Post Graduate School Monterey, CA 93940 Attn: Dr. E. R. Wood (Code 67)	1